Jerod C. Day
Mechanical and Energy Engineering,
University of North Texas,
Denton, TX 76203

Matthew K. Zemler
Mechanical Engineering,
Embry-Riddle Aeronautical University,
Daytona Beach, FL 32114

Matthew J. Traum
Mechanical Engineering,
Milwaukee School of Engineering,
Milwaukee, WI 53202

Sandra K. S. Boetcher[1]
Mechanical Engineering,
Embry-Riddle Aeronautical University,
Daytona Beach, FL 32114
e-mail: sandra.boetcher@erau.edu

Laminar Natural Convection From Isothermal Vertical Cylinders: Revisting a Classical Subject

Although an extensively studied classical subject, laminar natural convection heat transfer from the vertical surface of a cylinder has generated some recent interest in the literature. In this investigation, numerical experiments are performed to determine average Nusselt numbers for isothermal vertical cylinders ($10^2 < Ra_L < 10^9$, $0.1 < L/D < 10$, and $Pr = 0.7$) situated on an adiabatic surface in a quiescent ambient environment. Average Nusselt numbers for various cases will be presented and compared with commonly used correlations. Using Nusselt numbers for isothermal tops to approximate Nusselt numbers for heated tops will also be examined. Furthermore, the limit for which the heat transfer results for a vertical flat plate may be used as an approximation for the heat transfer from a vertical cylinder will be investigated. [DOI: 10.1115/1.4007421]

Keywords: laminar, natural convection, vertical cylinders, classic solutions, CFD

Introduction

Laminar natural convection heat transfer from the vertical surface of a cylinder is a classical subject, which has been studied extensively. When the boundary layer thickness δ is small compared to the diameter of the cylinder, Nusselt numbers may be determined by approximating the curved vertical surface as a flat plate. However, when the boundary layer thickness is large compared to the diameter of the cylinder, effects of curvature must be taken into account. Many investigators have studied the curvature limits for which the flat-plate model can be applied to estimate Nusselt numbers for vertical cylinders. Furthermore, these investigators have presented Nusselt number correlations for isothermal vertical cylinders.

In most heat transfer textbooks, including but not limited to Incropera et al. [1,2], Holman [3], Burmeister [4], and Gebhart et al. [5], the accepted limit for which the flat-plate solution can be used to approximate average Nusselt numbers for vertical cylinders ($\mathrm{Pr} = 0.72$) within 5% error is

$$\frac{D}{L} \geq \frac{35}{\mathrm{Gr}_L^{0.25}} \tag{1}$$

where D is the diameter of the cylinder, L is the height of the cylinder, and Gr_L is the Grashof number based on the height of the cylinder. This limit was derived by Sparrow and Gregg [6] in 1956 using a pseudosimilarity variable coordinate transformation and perturbation technique for solving the heat transfer and fluid flow adjacent to an isothermal vertical cylinder. They assumed the boundary layer thickness at the leading edge to be zero and they made use of the boundary layer approximation (all pressure gradients are zero and streamwise second derivatives are neglected) and Boussinesq approximation (density difference are small). In addition, Nusselt numbers for vertical cylinders ($\mathrm{Pr} = 0.72$ and 1; $0 < \xi < 1$) are presented as a truncated series solution and plotted. The curvature parameter ξ arose from a coordinate transformation done by Sparrow and Gregg [6] and is defined as

$$\xi = \frac{4L}{D}\left(\frac{\mathrm{Gr}_L}{4}\right)^{-1/4} \tag{2}$$

Around the same time as Sparrow and Gregg, LeFevre and Ede [7,8] solved the governing equations using the same assumptions as [6] with an integral method to obtain a correlation for vertical cylinder average Nusselt numbers, which is shown below

$$\mathrm{Nu}_L = \frac{4}{3}\left[\frac{7\mathrm{Gr}_L\mathrm{Pr}^2}{5(20+21\mathrm{Pr})}\right]^{1/4} + \frac{4(272+315\mathrm{Pr})L}{35(64+63\mathrm{Pr})D} \tag{3}$$

In this equation, Nu_L is the average Nusselt number and Pr is the Prandtl number.

In 1974, Cebeci [9] extended the work of Ref. [6] by numerically solving the governing equations using the boundary layer approximation for $0.01 \leq \mathrm{Pr} \leq 100$ and $0 < \xi < 5$. The results of Cebeci for the average Nusselt number for an isothermal vertical cylinder $\mathrm{Pr} = 0.72$ have been correlated in Popiel [10] with range of deviation from −0.34% −0.66%

$$\frac{\mathrm{Nu}_L}{\mathrm{Nu}_{L,\mathrm{fp}}} = 1 + 0.3\left[32^{0.5}\mathrm{Gr}_L^{-0.25}\frac{L}{D}\right]^{0.909} \tag{4}$$

In this equation, $\mathrm{Nu}_{L,\mathrm{fp}}$ is the average Nusselt number for the isothermal flat plate. Typically, the value for $\mathrm{Nu}_{L,\mathrm{fp}}$ is taken from the Churchill and Chu [11] correlations for natural convection from a vertical flat plate.

$$\mathrm{Nu}_{L,\mathrm{fp}} = 0.68 + \frac{0.670\mathrm{Ra}_L^{1/4}}{\left[1+(0.492/\mathrm{Pr})^{9/16}\right]^{4/9}} \tag{5}$$

In this equation, Ra_L is the Rayleigh number based on the height of the cylinder.

[1]Corresponding author.

Contributed by the Heat Transfer Division of ASME for publication in the Journal of Heat Transfer. Manuscript received December 26, 2011; final manuscript received August 13, 2012; published online January 3, 2013. Assoc. Editor: Giulio Lorenzini.

Also in 1974, Minkowycz and Sparrow [12] continued the work of Ref. [6] by investigating the impact of different levels of truncation in the series solution. Their findings indicate good agreement with Ref. [6] with a maximum deviation of 4% between the average Nusselt number solutions. They obtained results in graphical form for $0 < \xi < 10$ and for $\mathrm{Pr} = 0.733$.

In the late 1980s, Lee et al. [13] solved the boundary layer equations for nonuniform wall temperature using the similarity solution method. Their work extends that of Fujii and Uehara [14], except that unlike the authors of Ref. [14] who present information for local Nusselt numbers only, the authors of Ref. [13] present correlations for both the local and average Nusselt numbers for $0 < \xi < 70$. The average Nusselt number correlation in Ref. [13] for $0.1 \le \mathrm{Pr} \le 100$ when the wall temperature is uniform is reduced to

$$\ln\left[\mathrm{Nu}_L\left(\frac{\mathrm{Gr}_L}{4}\right)^{-\frac{1}{4}}\right] = F(\xi) + \left\{\ln\left[\mathrm{Nu}_{L,\mathrm{fp}}\left(\frac{\mathrm{Gr}_L}{4}^{-\frac{1}{4}}\right) + 2.92629\right]\right\} \times \exp(-G\xi^{1/2}) \tag{6}$$

and F and G are functions such that

$$F(\xi) = -2.92620 + 1.66850\xi^{1/2} - 0.21909\xi + 0.011308\xi^{3/2} \tag{7}$$

and

$$G = 0.29369 + 0.32635\mathrm{Pr}^{-0.19305} \tag{8}$$

with $\mathrm{Nu}_{L,\mathrm{fp}}$ being defined as

$$\mathrm{Nu}_{L,\mathrm{fp}}\left(\frac{\mathrm{Gr}_L}{4}\right)^{-1/4} = (2\mathrm{Pr})^{1/2}[2.5(1 + 2\mathrm{Pr}^{1/2} + 2\mathrm{Pr})]^{-1/4} \tag{9}$$

Although much classical work on the natural convection heat transfer from isothermal vertical cylinders has been reported, there has been recent interest in the subject as seen by a contemporary review article in 2008 on the subject by Popiel [10]. In 2003, Muñoz-Cobo et al. [15] studied power-law temperature distributions following on the work of Lee et al. [13]. In addition, several investigators have recently used either experimental means [16,17] or older analytical and numerical techniques [18] to study natural convection from a vertical cylinder.

Popiel et al. [17] conducted an experimental study on natural convection from an isothermal vertical cylinder. The investigators in Ref. [17], using the data reported in Ref. [9], propose a new limit for which the flat plate solution can be used to approximate the average Nusselt numbers with 3% error

$$\mathrm{Gr}_L^{0.25}\frac{D}{L} \le a + \frac{b}{\mathrm{Pr}^{0.5}} + \frac{c}{\mathrm{Pr}^2} \tag{10}$$

where $a = 11.474$, $b = 48.92$, and $c = -0.0006085$. Furthermore, experiments were conducted on an isothermal vertical cylinder with an insulated-top situated on an insulated surface for $\mathrm{Pr} = 0.71, 1.5 \times 10^8 < \mathrm{Ra}_L < 1.1 \times 10^9$, and $0 < L/D < 60$. The results of this study were correlated into the following equation:

$$\mathrm{Nu}_L \le A\mathrm{Ra}_L^n \tag{11}$$

where

$$A = 0.519 + 0.03454\frac{L}{D} + 0.0008772\left(\frac{L}{D}\right)^2 + 8.855 \times 10^{-6}\left(\frac{L}{D}\right)^3 \tag{12}$$

and

$$n = 0.25 - 0.00253\frac{L}{D} + 1.152 \times 10^{-5}\left(\frac{L}{D}\right)^2 \tag{13}$$

Their results agree fairly well with Cebeci [9] for the higher Rayleigh numbers which were studied.

In the majority of the work done on natural convection heat transfer from vertical cylinders, the top of the cylinder is usually assumed to be adiabatic. Despite the vast amounts of literature available, to the best knowledge of the authors, very few investigators have studied the effect of a heated top on the average Nusselt number. In 1978, Oosthuizen [19] examined the effect of cylinders having heated exposed ends on the average Nusselt number. In general, he found that the average Nusselt numbers for the heated ends was up to 30% lower in some cases compared to the equivalent cylinder with an adiabatic end.

Very recently, Eslami and Jafarpur [20] (who built upon the previous work of several other studies [21–24]) investigated laminar natural convection from isothermal cylinders with active ends. These authors present a generalized semiempirical method to calculate average Nusselt numbers from arbitrary shapes in which they use to present results for specific geometric cases, including vertical cylinders. The generalized equation for the Nusselt number for a vertical cylinder with one active end (heated top) based on the square-root of the area is

$$\mathrm{Nu}_{\sqrt{A}} = \mathrm{Nu}_{\sqrt{A}}^0 + f(\mathrm{Pr})G_{\mathrm{dyn}}\mathrm{Ra}_{\sqrt{A}}^{1/4} \tag{14}$$

where $f(\mathrm{Pr})$ is the Prandtl function

$$f(\mathrm{Pr}) = \frac{0.670}{[1 + 0.5/\mathrm{Pr})^{9/16}]^{4/9}} \tag{15}$$

and they dynamic gravity function is defined as

$$G_{\mathrm{dyn}} = \frac{\mathrm{BFF} + \frac{G_{\mathrm{up}}}{G_{\mathrm{low}}}\mathrm{Ra}_{\sqrt{A}}^{1/4}}{\mathrm{BFF} + C \cdot \mathrm{Ra}_{\sqrt{A}}^{1/4}} C \cdot G_{\mathrm{low}} \tag{16}$$

where the body force function is

$$\mathrm{BFF} = \frac{\mathrm{Nu}_{\sqrt{A}}^0}{f(\mathrm{Pr}) \cdot G_{\mathrm{low}}} \tag{17}$$

$$C = 0.34 + 0.046 \cdot \mathrm{BFF} \tag{18}$$

and the lower-bound and upper-bound gravity force functions specifically for a vertical cylinder with one heated end are

$$G_{\mathrm{low}} = \left[0.952^{4/3} \times \left(\frac{\pi D^2/4}{\pi D^2/4 + \pi DL}\right)^{7/6} + (1.154(D/L)^{1/8})^{4/3} \times \left(\frac{\pi DL}{\pi D^2/4 + \pi DL}\right)^{7/6}\right]^{3/4} \tag{19}$$

$$G_{\mathrm{up}} = 0.952 \times \left(\frac{\pi D^2/4}{\pi D^2/4 + \pi DL}\right)^{7/8} + 1.154(D/L)^{1/8} \times \left(\frac{\pi DL}{\pi D^2/4 + \pi DL}\right)^{7/8} \tag{20}$$

The conduction limit for circular cylinders $0 \leq L/D \leq 8$ is

$$\mathrm{Nu}^0_{\sqrt{A}} = \frac{8.00 + 6.95(L/D)^{0.76}}{\left(2\pi + 4\pi(L/D)\right)^{1/2}} \tag{21}$$

The Nusselt numbers based on the square-root of the area were converted to Nusselt numbers based on the height (L) of the cylinders when later compared to the results of the present study.

High-quality natural convection heat transfer experiments that correctly interrogate heated shapes in air are inherently difficult to perform, which is reflected in the lack of experimental data available in the literature. Much analytical and numerical work is inconsistent due to the practices of (1) neglecting the streamwise second derivative in the Navier–Stokes equation (i.e., using boundary layer approximation), (2) using boundary conditions that are not representative of the space surrounding real objects, and (3) method of solution (integral, pseudosimilarity, finite-difference). Previous work typically places the boundary at the top of the cylinder instead of considering the effect of the resulting plume on the boundary layer of the vertical surface. In addition, the majority of previous investigators ignored the effect of a heated top in the calculation of the average Nusselt numbers.

The goal of this work is to perform numerical experiments which take into account the streamwise second derivatives in the governing equations and allow for full plume growth to determine average Nusselt numbers for laminar isothermal vertical cylinders ($10^2 < \mathrm{Ra}_L < 10^9, 0.1 < L/D < 10$, and $\mathrm{Pr} = 0.7$) situated on an adiabatic surface in a quiescent ambient environment. The results will be compared against all other known classical solutions for isothermal vertical cylinders. Furthermore, the validity of Eqs. (1) and (10) for determining the range at which the flat-plate solution may be used as an approximation for a vertical cylinder will be investigated. Finally, the effect of ignoring a heated top on the average Nusselt numbers will be shown.

Problem Formulation

Physical Model and Solution Domain. Consider a vertical cylinder with isothermal walls and an adiabatic or heated top of diameter D and height L situated on an adiabatic surface in a quiescent, constant-temperature ambient environment. The top will either be adiabatic in order to investigate the accuracy of the classical sidewall solutions, or isothermal (heated top) in order to compare against the adiabatic-top case. Due to both geometric and thermal axisymmetry, this problem may be modeled as two-dimensional. The solution domain is presented in Fig. 1.

In Fig. 1, r and z are the radial and axial coordinates, respectively. Furthermore, W is the width of the solution domain which is set to 5D and H is the height of the solution domain which is equal to (24D + L). The aspect ratio of the cylinder AR = L/D is varied parametrically, $0.1 \leq \mathrm{AR} \leq 10$.

Governing Equations. The subsequent dimensionless variables are used in writing the governing equations

$$R = \frac{r}{L}, \quad Z = \frac{z}{L}, \quad U_R = \frac{u_r}{\nu/L}, \quad U_Z = \frac{u_z}{\nu/L},$$
$$\theta = \frac{T - T_\infty}{T_{\mathrm{cylinder}} - T_\infty}, \quad P = \frac{p - p_\infty}{\rho(\nu/L)^2} \tag{22}$$

and

$$\mathrm{Gr}_L = \frac{g\beta(T_{\mathrm{cylinder}} - T_\infty)L^3}{\nu^2}, \quad \mathrm{Pr} = \frac{c_p\mu}{k} \tag{23}$$

Here, r and z are the radial and axial coordinates, respectively, u_r and u_z are the radial and axial velocity components, ν is the kinematic viscosity, T is the temperature, T_{cylinder} is the temperature at the wall of the cylinder, T_∞ is the ambient temperature far from the cylinder, p is the local pressure, p_∞ is the freestream pressure, g is gravity, β is the coefficient of thermal expansion, c_p is the specific heat at constant pressure, μ is the dynamic viscosity, and k is the thermal conductivity. All thermal properties are assumed to be constant and Pr = 0.7.

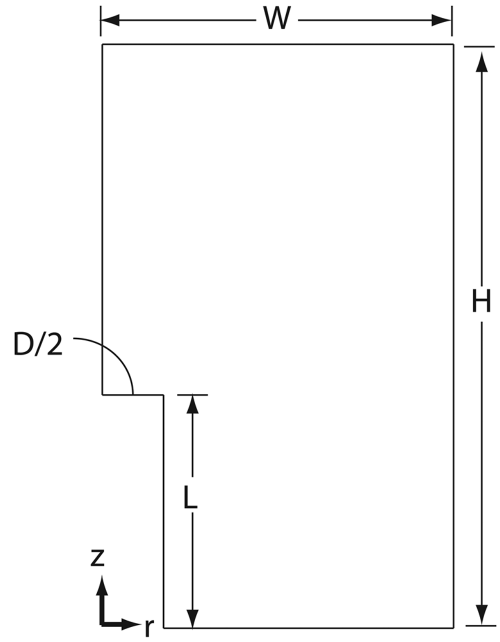

Fig. 1 Schematic diagram of the solution domain

The governing equations for axisymmetric, laminar, incompressible, natural convection flow are

Conservation of mass

$$\frac{1}{R}\frac{\partial(RU_R)}{\partial R} + \frac{\partial(U_Z)}{\partial Z} = 0 \tag{24}$$

Conservation of momentum in the Z-direction

$$U_R\frac{\partial U_Z}{\partial R} + U_Z\frac{\partial U_Z}{\partial Z} = -\frac{\partial P}{\partial Z} + \frac{1}{R}\frac{\partial}{\partial R}R\frac{\partial U_Z}{\partial R} + \frac{\partial^2 U_Z}{\partial Z^2} + \mathrm{Gr}_L\theta \tag{25}$$

Conservation of momentum in the R-direction

$$U_R\frac{\partial U_R}{\partial R} + U_Z\frac{\partial U_R}{\partial Z} = -\frac{\partial P}{\partial R} + \frac{1}{R}\frac{\partial}{\partial R}R\frac{\partial U_R}{\partial R} + \frac{\partial^2 U_R}{\partial Z^2} - \frac{U_R}{R^2} \tag{26}$$

Conservation of energy

$$U_R\frac{\partial \theta}{\partial R} + U_Z\frac{\partial \theta}{\partial Z} = \frac{1}{\mathrm{Pr}}\left[\frac{1}{R}\frac{\partial}{\partial R}R\frac{\partial \theta}{\partial R} + \frac{\partial^2 \theta}{\partial Z^2}\right] \tag{27}$$

The Boussinesq approximation can be employed here due to negligible density differences. The viscous dissipation and work terms can be neglected in the energy equation because of the small velocities encountered in natural convection flow.

Boundary Conditions. The temperature at the vertical surface of the cylinder is T_{cylinder} and the no-slip condition is applied. The boundary conditions at the surface of the cylinder in dimensionless form are

$$U_R = U_Z = 0 \quad \text{and} \quad \theta = 1 \tag{28}$$

The top surface of the cylinder is either adiabatic

$$\frac{\partial \theta}{\partial Z} = 0 \tag{29}$$

or isothermal

$$\theta = 1 \tag{30}$$

In both of these cases, no-slip applies

$$U_R = U_Z = 0 \tag{31}$$

On the bottom surface of the fluid domain, adiabatic and no-slip boundary conditions are applied such that

$$U_R = U_Z = 0 \quad \text{and} \quad \frac{\partial \theta}{\partial Z} = 0 \tag{32}$$

Along the axis of symmetry ($R = 0$) the boundary conditions are

$$U_R = \frac{\partial U_Z}{\partial R} = \frac{\partial \theta}{\partial R} = 0 \tag{33}$$

Relatively weak boundary conditions (the so-called opening condition in ANSYS CFX) are placed at the far-field boundaries at the top and side of the solution domain. The conditions allow the flow to either entrain into the domain or flow out. Specified at these boundaries are the pressure and the temperature of the fluid if entering into the domain.

At the top of the solution domain

$$P = 0 \quad \text{and} \quad \theta = 0 \quad \text{if} \quad U_Z < 0 \tag{34}$$

Along the side of the solution domain

$$P = 0 \quad \text{and} \quad \theta = 0 \quad \text{if} \quad U_R < 0 \tag{35}$$

Solution

ANSYS CFX 12.0, a finite-volume-based computational fluid dynamics solver, was used to perform the numerical experiments. Unlike the classical methods of using the integral method, solving for the boundary layer equations, using semiempirical analysis, and/or perturbation techniques, ANSYS CFX 12.0 solves for the full conservation of mass, momentum, and energy equations. Furthermore, in the numerical approach here, solution domain boundaries are extended further out minimizing boundary condition assumptions in the area of the flow (i.e., the plume at the top of the cylinder is allowed to grow, whereas in the classical solutions, the boundary is cut-off at the top of the cylinder).

The number of nodes used was 210,000. Mesh independence was established by multiplying the number of nodes by two. The average Nusselt numbers of the two meshes varied by less than 0.3%.

The boundaries of the solution domain were placed far enough away as to not affect the solution of the area of interest, in this case, the heat transfer at the cylinder. In order to make sure that the boundaries did not interfere with the heat transfer results, the height and width of the solution domain were varied and tested.

Results and Discussion

Adiabatic Top. Results will now be presented to compare the current work ($Pr = 0.7$) to other classical solutions ($Pr \approx 0.7$) for laminar natural convection from an isothermal cylinder with an adiabatic top.

Figures 2–10 have been prepared to show the average Nusselt numbers versus Rayleigh number for several different aspect

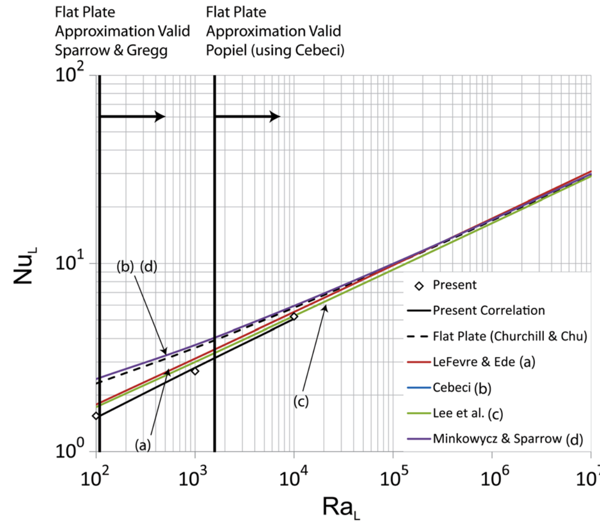

Fig. 2 Insulated-top average Nusselt number versus Rayleigh number for AR = 0.1

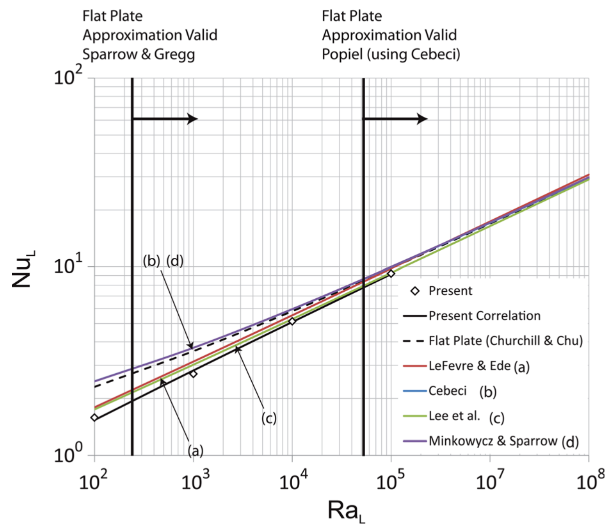

Fig. 3 Insulated-top average Nusselt number versus Rayleigh number for AR = 0.125

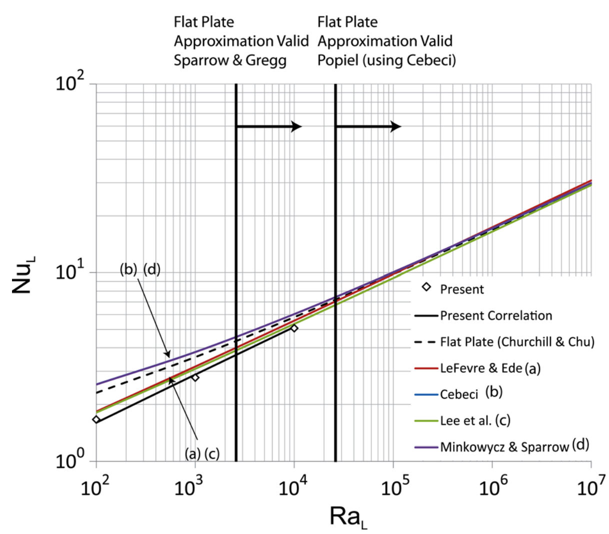

Fig. 4 Insulated-top average Nusselt number versus Rayleigh number for AR = 0.2

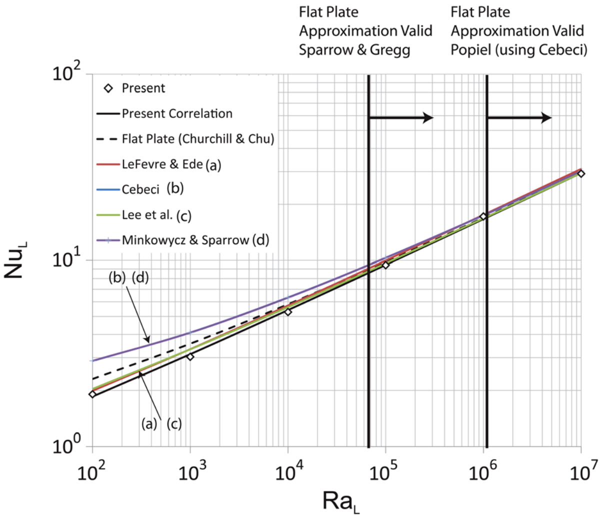

Fig. 5 Insulated-top average Nusselt number versus Rayleigh number for AR = 0.5

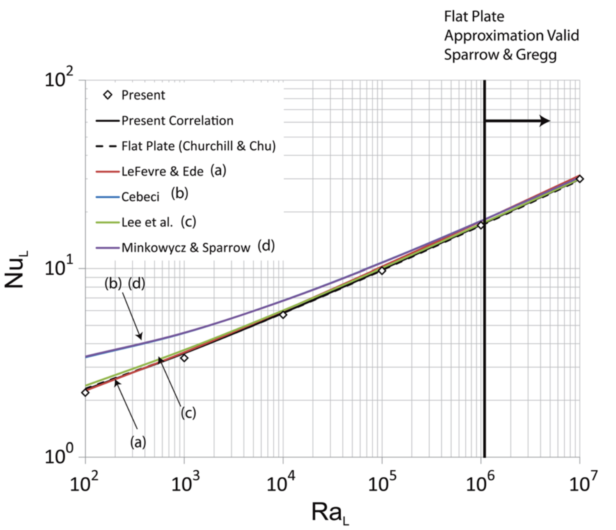

Fig. 6 Insulated-top average Nusselt number versus Rayleigh number for AR = 1

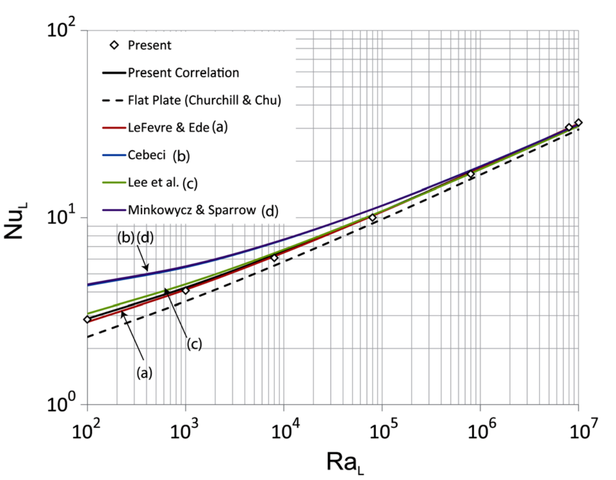

Fig. 7 Insulated-top average Nusselt number versus Rayleigh number for AR = 2

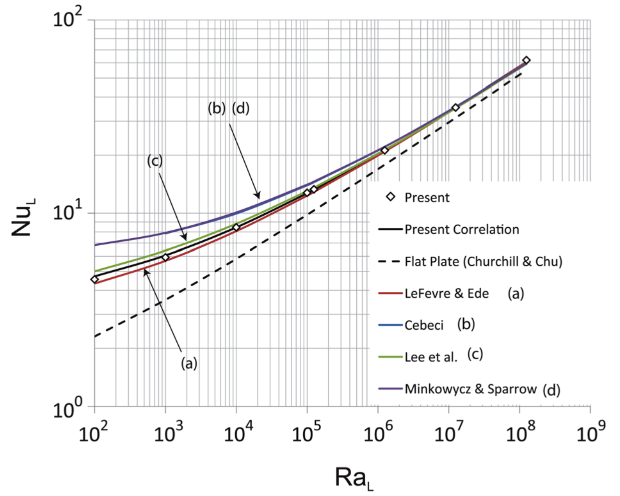

Fig. 8 Insulated-top average Nusselt number versus Rayleigh number for AR = 5

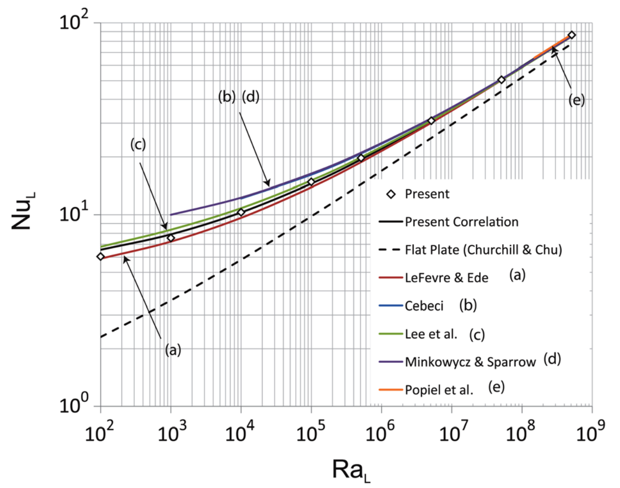

Fig. 9 Insulated-top average Nusselt number versus Rayleigh number for AR = 8

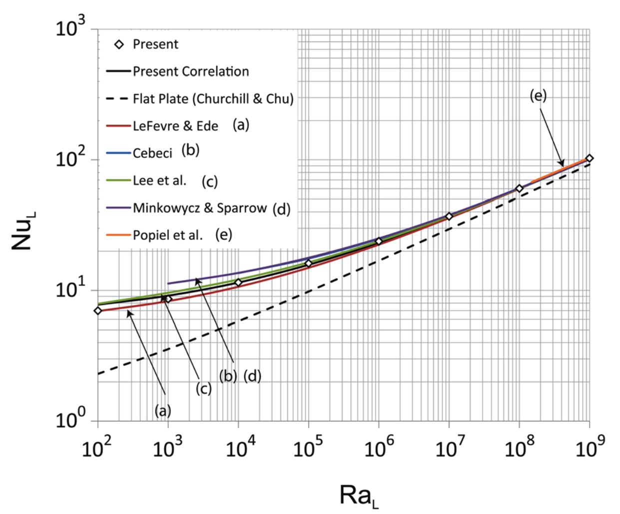

Fig. 10 Insulated-top average Nusselt number versus Rayleigh number for AR = 10

ratios. The current numerical experiments (Present) are compared with previous work by LeFevre and Ede [7,8]—Eq. (3), Cebeci [9]—Eq. (4), Minkowycz and Sparrow [12], Lee et al. [13]—Eqs. (6)–(9), Popiel [10]—Eqs. (10)–(13), and the isothermal laminar vertical flat plate correlation from Churchill and Chu [11]—Eq. (5). Furthermore, the present data have been correlated into an equations for $\mathrm{Pr} = 0.7$ and plotted in the figures. The resulting correlation was developed using the MATLAB surface fitting tool using a nonlinear least squares method with a least absolute residuals robust algorithm and are presented below. The R-squared value was 0.9999.

For $0.1 \leq \mathrm{AR} \leq 1$

$$\mathrm{Nu}_L = -0.2165 + 0.5204\mathrm{Ra}_L^{1/4} + 0.8473\left[\frac{L}{D}\right] \tag{36}$$

For $2 \leq \mathrm{AR} \leq 10$

$$\mathrm{Nu}_L = -0.06211 + 0.54414\mathrm{Ra}_L^{1/4} + 0.6123\left[\frac{L}{D}\right] \tag{37}$$

The applicability limits of vertical flat-plate solution as an approximation of the average heat transfer coefficient for an isothermal vertical cylinder are shown in Figs. 2–6 by solid vertical black lines (for Figs. 7–10, the limits are located at Ra_L greater than those of interest). These figures include the range proposed by Sparrow and Gregg [6] (Eq. (1)) (within 5% of flat plate) and the more conservative estimate provided by Popiel using the data of Cebeci [9,10] (Eq. (10)) (within 3% of flat plate).

As the Rayleigh number increases, all solutions asymptotically approach the flat-plate solution. As the aspect ratio increases, the cut-off Rayleigh number for which the flat-plate solution can be used to approximate the Nusselt number increases.

For $\mathrm{AR} = 0.1$, Sparrow and Gregg claim that the flat-plate solution can be used to approximate Nusselt numbers for Ra_L greater than 100. However, upon inspection of Fig. 2, the present solution deviates from that of the flat plate by a much as 32%. Furthermore, the present solution deviates from that of Minkowycz and Sparrow (virtually the exact same results as Cebeci) by upwards of 36%. It is interesting to note, that the solutions of LeFevre and Ede were determined using an integral method, yet the deviation from that solution and the present solution is approximately 13%. Furthermore, the solutions of Lee et al. are very close to that of LeFevre and Ede. Extrapolation of results for $\mathrm{AR} = 0.1$ places the limit at $\mathrm{Ra}_L \approx 10^5$ for 5% deviation from the flat plate.

Figures 3–6 present similar stories. The present data are closer to that of LeFevre and Ede than it is to Minkowycz and Sparrow (Cebeci); and the higher the aspect ratio, the closer the present solution is to LeFevre and Ede. Also observed is that the higher the aspect ratio, the closer the present solution (and LeFevre and Ede) approaches that of the flat-plate solution in this range of aspect ratios ($0.1 \leq \mathrm{AR} \leq 1$). Interestingly, the reverse trend is seen in the data of Minkowycz and Sparrow (Cebeci)—as the aspect ratio increases, the data get farther away from the flat-plate solution, which is evidenced by the approximation line increasing in Rayleigh number.

At one end of the aspect ratio spectrum ($\mathrm{AR} = 0.1$), according to the data of LeFevre and Ede, Lee et al., and the present work, the Sparrow and Gregg limit is at a too low of a Rayleigh number. However, when $\mathrm{AR} = 1$, according to the data of LeFevre and Ede, Lee et al., and the present work, the Sparrow and Gregg limit predicts the valid usage of the flat-plate approximation at too high of a Rayleigh number.

For $\mathrm{AR} = 0.125$, the limit can be placed at $\mathrm{Ra}_L \approx 10^5$ for 6% deviation from the flat plate. Extrapolating, for $\mathrm{AR} = 0.2$, Nusselt numbers deviate approximately 5% at $\mathrm{Ra}_L \approx 10^5$. For $\mathrm{AR} = 0.5$ and $\mathrm{AR} = 1$, the limit can be placed at $\mathrm{Ra}_L \approx 10^5$ and $\mathrm{Ra}_L \approx 10^3$ for 4% and 6% deviations, respectively.

Next, attention will be turned to Figs. 7–10. In this group of aspect ratios (which are representing more tall, slender cylinders: $2 \leq \mathrm{AR} \leq 10$), there is no question that any of the solutions can be approximated using the flat plate. Here, the results of LeFevre and Ede and Lee et al. differ slightly more, with the present solution found in between these two. For $\mathrm{AR} = 2$, the present results differ from Minkowycz and Sparrow (Cebeci) by as much as 34%. As the aspect ratios increase, the percent difference between all of the solutions decreases. As an aside, for $\mathrm{AR} = 8$ and 10, the lower Rayleigh numbers are out of the range of curvature parameters for which the Minkowycz and Sparrow (Cebeci) solutions are valid ($0 < \xi < 10$) and are therefore not plotted.

It is of particular interest to note that in many heat transfer textbooks, including Refs. [1–3], after being instructed to determine whether curvature effects are important using Eq. (1), the reader is directed to use the results of Refs. [6,9], and/or [12], which are the results from Sparrow, Gregg, Minkowycz and Cebeci.

Heated Top. As was mentioned in the Introduction, very little work has been presented on natural convection from vertical cylinders with heated tops. Oosthuizen [19] included in his work the case of an isothermal cylinder situated upright on an adiabatic base with a heated top (like the present). Oosthuizen's experimental data include only 11 data points, two of which fall under the same aspect ratios simulated here $\mathrm{AR} = 1$ and 2. Eslami and Jafarpur [20] presented the case of an isothermal cylinder with both ends (top and bottom) active. In the present manuscript, the generalized equations presented in Ref. [20] were used to determine the average Nusselt numbers for an isothermal cylinder with only the side and top heated and have included this data with the present results (details in the Introduction).

Similar to the adiabatic case, the present data were correlated using the same method and plotted using the following equations.

For $0.1 \leq \mathrm{AR} \leq 0.2$

$$\mathrm{Nu}_L = -0.2823 + 0.2657\mathrm{Ra}_L^{1/4} + 3.657\left[\frac{L}{D}\right] \tag{38}$$

For $\mathrm{AR} = 0.5$

$$\mathrm{Nu}_L = -128.3 + 0.3692\mathrm{Ra}_L^{1/4} + 64.7\left[\frac{L}{D}\right] \tag{39}$$

For $\mathrm{AR} = 1$

$$\mathrm{Nu}_L = 0.1557 + 0.4718\mathrm{Ra}_L^{1/4} + 0.315\left[\frac{L}{D}\right] \tag{40}$$

For $2 \leq \mathrm{AR} \leq 10$

$$\mathrm{Nu}_L = -0.3903 + 0.5399\mathrm{Ra}_L^{1/4} + 0.6367\left[\frac{L}{D}\right] \tag{41}$$

As the aspect ratio decreases, the vertical cylinder looks increasingly more like an isothermal horizontal disk. Therefore, careful attention must be paid to the laminar-turbulent transition Rayleigh number for a heated horizontal disk. According to recent experiments by Kitamura and Kimura [25], the transitional diameter-based Rayleigh number Ra_D for air lies between 1 and 2×10^6. All Nusselt numbers presented here are for $\mathrm{Ra}_D \leq 1 \times 10^6$, when the cylinder height-based Rayleigh number Ra_L is converted to a diameter-based Rayleigh number.

Since at low aspect ratios, the vertical cylinder looks like a thin, horizontal heated disk, a well-validated empirical correlation proposed by Kobus and Wedekind [26] for the average Nusselt number for isothermal upward-facing horizontal disks in air will be plotted for $\mathrm{AR} < 1$. The correlation is reproduced below.

For $3 \times 10^2 \leq \mathrm{Ra}_D \leq 10^4$

$$\mathrm{Nu}_D = 1.759\mathrm{Ra}_D^{0.130} \tag{42}$$

and for $10^4 \leq \mathrm{Ra}_D \leq 3 \times 10^7$

$$\mathrm{Nu}_D = 0.9724\mathrm{Ra}_D^{0.194} \quad (43)$$

Although presenting the data for an upward-facing horizontal disk in terms of the diameter-based Rayleigh and Nusselt numbers makes more sense, the diameter-based Nusselt numbers for the correlation will be converted into height-based Nusselt numbers so that they may be plotted on the figures for comparison purposes.

Figures 11–19 show present results for both the adiabatic- and heated-top cases for varying Rayleigh numbers and aspect ratios. Results using the technique of Eslami and Jafarpur (except for AR = 10 since that fell out of the range of applicability of the equations) are plotted. The two experimental data points of Oosthuizen are plotted for AR = 1 and 2 in Figs. 15 and 16, and the horizontal isothermal disk correlation is shown for AR < 1 (Figs. 11–14).

Like Oosthuizen reported, the average Nusselt numbers for the heated top are lower than that for the adiabatic top. Solutions from Eslami and Jafarpur fall between the adiabatic- and heated-top cases for the lower aspect ratios (AR $\leq$ 0.2) and line up with the insulated-top case for AR $\geq$ 0.5. The Eslami and Jafarpur solutions deviate at low values of the Rayleigh number, perhaps suggesting a Rayleigh-number limit for their solution. The Oosthuizen data points appear to be outliers on the graphs with an approximately 40% deviation for AR = 1 and 5% deviation for AR = 2.

Of further interest is the good agreement of the heated-top case with the horizontal disk correlation for the average Nusselt

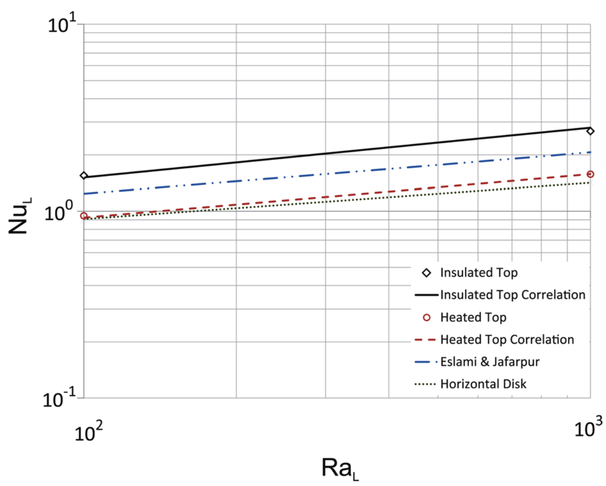

Fig. 11 Comparison of average Nusselt number versus Rayleigh number for AR = 0.1

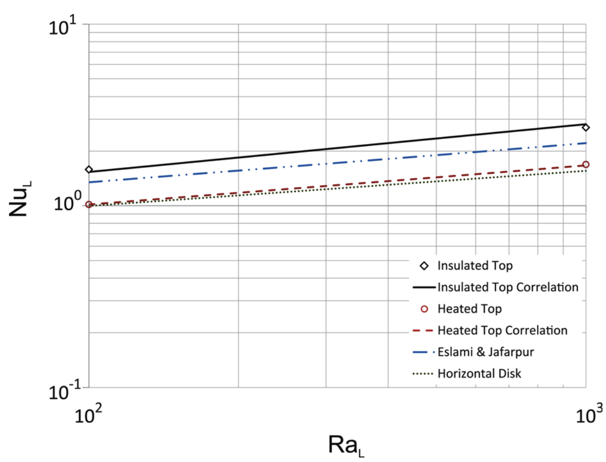

Fig. 12 Comparison of average Nusselt number versus Rayleigh number for AR = 0.125

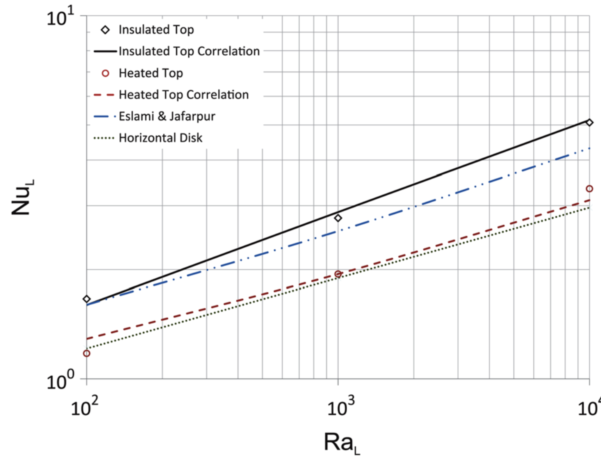

Fig. 13 Comparison of average Nusselt number versus Rayleigh number for AR = 0.2

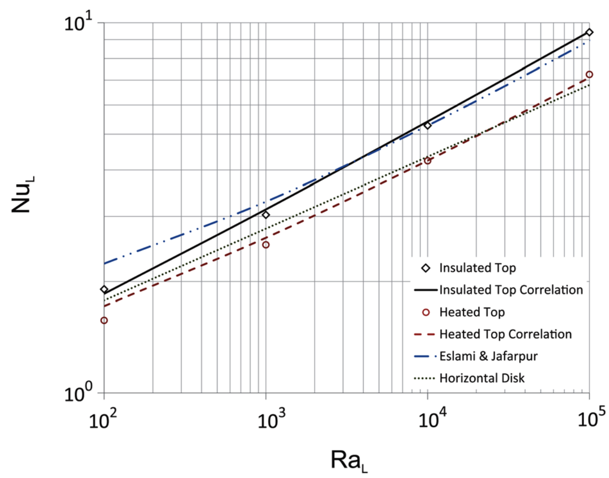

Fig. 14 Comparison of average Nusselt number versus Rayleigh number for AR = 0.5

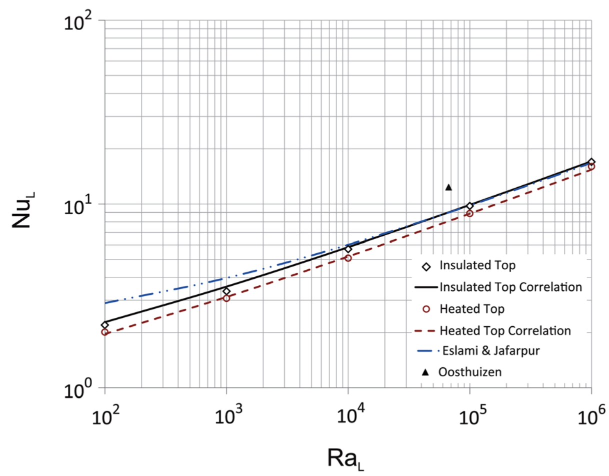

Fig. 15 Comparison of average Nusselt number versus Rayleigh number for AR = 1

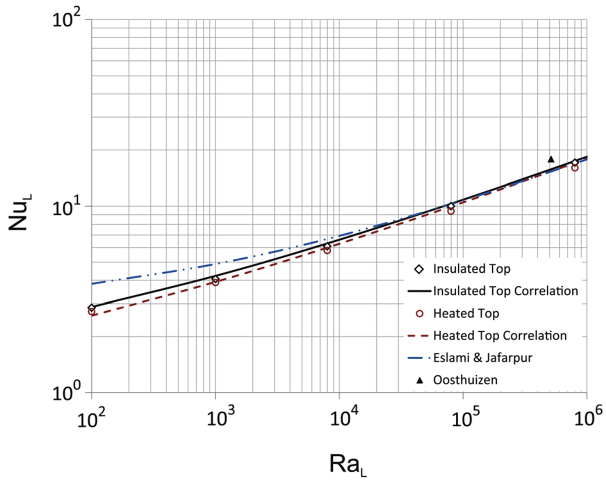

Fig. 16 Comparison of average Nusselt number versus Rayleigh number for AR = 2

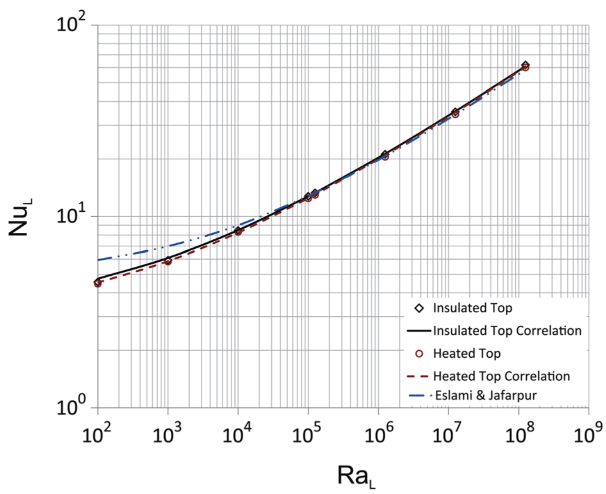

Fig. 17 Comparison of average Nusselt number versus Rayleigh number for AR = 5

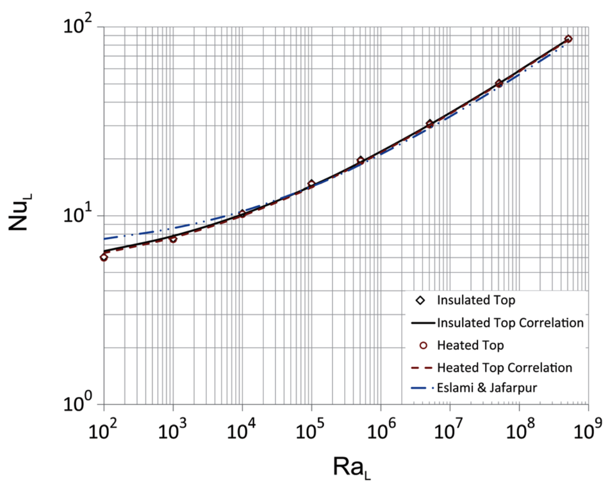

Fig. 18 Comparison of average Nusselt number versus Rayleigh number for AR = 8

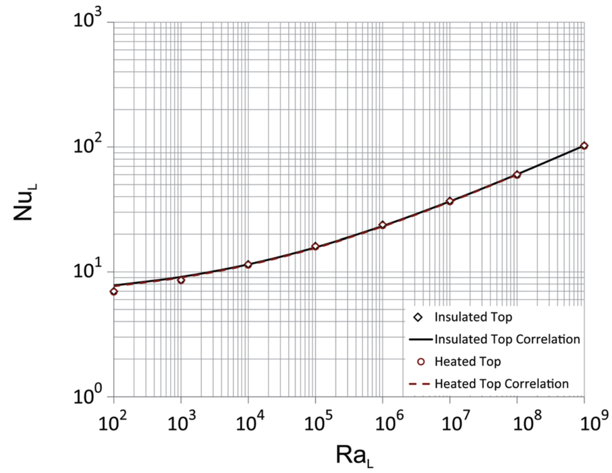

Fig. 19 Comparison of average Nusselt number versus Rayleigh number for AR = 10

numbers, which helps validate the claim that as the aspect ratio decreases, the vertical cylinder with a heated top looks more like a thin heated disk from a heat transfer perspective. For AR = 0.1, the maximum percent difference between the heated-top case and the horizontal disk is approximately 5%. As the aspect ratio increases, the percent difference increases slightly. It is also interesting to note that the Eslami and Jafarpur results, although experimentally validated for L/D = 0.1 and 0.5, do not agree with either the present solution or Kobus and Wedekind.

The percent difference between the insulated-top case and the heated-top case remains relatively constant for all values of the Rayleigh numbers for a given aspect ratio, and as the aspect ratio increase, the percent difference decreases. For AR = 0.1, the percent difference between the two is around 40%, for AR = 1, the difference is 10%, and for AR = 10, the percent difference is on the order of 1%. Nusselt numbers for heated-top cylinders with aspect ratios greater than 2 can be approximated using the adiabatic-top solution to within 5%.

Concluding Remarks

In the present study, numerical experiments have been performed to interrogate the average natural convection Nusselt numbers for laminar isothermal vertical cylinders situated on an adiabatic surface in a quiescent ambient environment for $\mathrm{Pr} = 0.7, 10^2 < \mathrm{Ra}_L < 10^9$, and $0.1 < L/D < 10$. From the results, a new average Nusselt number correlation was developed. The case where the top of the cylinder is adiabatic was compared to several other frequently cited classical solutions found in heat transfer textbooks, as well as other solutions less cited. It was found that the highly cited classical solutions (Minkowycz and Sparrow, Cebeci) were not always in agreement with the present solution or the other less-cited vertical cylinder solutions (LeFevre and Ede, Lee et al.). Furthermore, the limit for which the average Nusselt numbers for the flat-plate solution may be used as an approximation for the vertical cylinder (which, again, is referenced in all commonly used heat transfer textbooks) did not agree with the data of LeFevre and Ede, Lee et al., or the present investigation.

The case where the cylinder has a heated top has received less attention. Results from the present study show that the average Nusselt numbers for the heated top are less than that for the adiabatic top. Also, when the aspect ratio is low, the Nusselt numbers agree more with the upward-facing isothermal disk; and when the aspect ratio is high, the average Nusselt number approaches that of the average Nusselt number for an isothermal vertical cylinder with an adiabatic top. A correlation for isothermal cylinders with heated tops is proposed and results are compared with known investigations (including a very recent study). Further analytical and experimental data for cylinders with heated tops and thin horizontal heated disks are needed.

Nomenclature

A = coefficient/area
a = coefficient
AR = aspect ratio, L/D
b = coefficient
BFF = body force function
C = constant
c = coefficient
c_p = specific heat at constant pressure
D = diameter of the cylinder
F = function
f = function
G = function
g = gravitational constant
G_{dyn} = dynamic gravity function
G_{low} = lower-bound gravity function
G_{up} = upper-bound gravity function
$\mathrm{Gr}_{\sqrt{A}}$ = Grashof number, $g\beta(T_{\mathrm{cylinder}}-T_\infty)\sqrt{A}^3/\nu^2$
Gr_D = Grashof number, $g\beta(T_{\mathrm{cylinder}}-T_\infty)D^3/\nu^2$
Gr_L = Grashof number, $g\beta(T_{\mathrm{cylinder}}-T_\infty)L^3/\nu^2$
H = height of solution domain
$\bar{h}$ = aspect ratio, L/D
k = thermal conductivity
L = height of cylinder
n = coefficient
$\mathrm{Nu}_{\sqrt{A}}$ = average Nusselt number, $\bar{h}\sqrt{A}/k$
$\mathrm{Nu}^0_{\sqrt{A}}$ = conduction limit
Nu_L = average Nusselt number, $\bar{h}L/k$
$\mathrm{Nu}_{L,\mathrm{fp}}$ = average Nusselt number of flat plate
P = dimensionless pressure, $(P-P_\infty)/\rho(\nu D)^2$
p = pressure
p_∞ = free-stream pressure
Pr = Prandtl number, $c_p\mu/k$
R, Z = dimensionless cylindrical coordinates, $(r,z)/D$
r, z = cylindrical coordinates
Ra_D = Rayleigh number, $\mathrm{Gr}_D\mathrm{Pr}$
Ra_L = Rayleigh number, $\mathrm{Gr}_L\mathrm{Pr}$
T = temperature
T_{cylinder} = temperature at the vertical surface of the cylinder
T_∞ = temperature of the ambient environment
U_R, U_Z = dimensionless velocity components, $(u_r, u_z)/(\nu/D)$
W = width of solution domain

Greek Symbols

β = isobaric coefficient of thermal expansion
δ = boundary layer thickness
θ = dimensionless temperature, $(T-T_\infty)/(T_{\mathrm{cylinder}}-T_\infty)$
μ = dynamic viscosity of the fluid
ν = kinematic viscosity of the fluid
ξ = curvature parameter, $(4L/D)(\mathrm{Gr}_L/4)^{-1/4}$
ρ = density of the fluid

References

[1] Incropera, F. P., Dewitt, D. P., Bergman, T. L., and Lavine, A. S., 2007, *Introduction to Heat Transfer*, 5th ed., John Wiley & Sons, Inc., Hoboken, NJ.
[2] Incropera, F. P., Dewitt, D. P., Bergman, T. L., and Lavine, A. S., 2007, *Fundamentals of Heat and Mass Transfer*, 6th ed., John Wiley & Sons, Inc., Hoboken, NJ.
[3] Holman, J. P., 2010, *Heat Transfer*, 10th ed., McGraw-Hill Companies, Inc., New York.
[4] Burmeister, L., 1993, *Convective Heat Transfer*, 2nd ed., John Wiley & Sons, Inc, New York.
[5] Gebhart, B., Jaluria, Y., Mahajan, R. L., and Sammakia, B., 1988, *Buoyancy-Induced Flows and Transport: Reference Edition*, Hemisphere Publishing Company, New York.
[6] Sparrow, E. M., and Gregg, J. L., 1956, "Laminar-Free-Convection Heat Transfer From the Outer Surface of a Vertical Circular Cylinder," Trans. ASME, **78**, pp. 1823–1829.
[7] LeFevre, E. J., and Ede, A. J., 1956, "Laminar Free Convection From the Outer Surface of a Vertical Cylinder," Proceedings of the 9th International Congress on Applied Mechanics, pp. 175–183.
[8] Ede, A. J., 1967, "Advances in Free Convection," *Advances in Heat Transfer*, Academic Press, New York, pp. 1–64.
[9] Cebeci, T., 1974, "Laminar-Free-Convective-Heat Transfer From the Outer Surface of a Vertical Circular Cylinder," Proceedings of the 5th International Heat Transfer Conference, Tokyo, pp. 1–64.
[10] Popiel, C. O., 2008, "Free Convection Heat Transfer From Vertical Slender Cylinders: A Review," Heat Transfer Eng., **29**, pp. 521–536.
[11] Churchill, S. W., and Chu, H. H. S., 1975, "Correlating Equations for Laminar and Turbulent Free Convection From a Vertical Plate," Int. J. Heat Mass Transfer, **18**, pp. 1323–1329.
[12] Minkowycz, W. J., and Sparrow, E. M., 1974, "Local Nonsimilar Solutions for Natural Convection on a Vertical Cylinder," ASME J. Heat Transfer, **96**, pp. 178–183.
[13] Lee, H. R., Chen, T. S., and Armaly, B. F., 1988, "Natural Convection Along Slender Vertical Cylinders With Variable Surface Temperature," ASME J. Heat Transfer, **110**, pp. 103–108.
[14] Fujii, T., and Uehara, H., 1970, "Laminar Natural-Convective Heat Transfer From the Outside of a Vertical Cylinder," Int. J. Heat Mass Transfer, **13**, pp. 607–615.
[15] Muñoz-Cobo, J. L., Corberán, J. M., and Chiva, S., 2003, "Explicit Formulas for Laminar Natural Convection Heat Transfer Along Vertical Cylinders With Power-Law Wall Temperature Distribution," Heat Mass Transfer, **39**, pp. 215–222.
[16] Kimura, F., Tachibana, T., Kitamura, K., and Hosokawa, T., 2004, "Fluid Flow and Heat Transfer of Natural Convection Around Heated Vertical Cylinders (Effect of Cylinder Diameter)," JSME Int. J. Ser. B, **47**, pp. 159–161.
[17] Popiel, C. O., Wojtkowiak, J., and Bober, K., 2007, "Laminar Free Convective Heat Transfer From Isothermal Vertical Slender Cylinders," Exp. Therm. Fluid Sci., **32**, pp. 607–613.
[18] Gori, F., Serrano, M. G., and Wang, Y., 2006, "Natural Convection Along a Vertical Thin Cylinder With Uniform and Constant Wall Heat Flux," Int. J. Thermophys., **27**, pp. 1527–1538.
[19] Oosthuizen, P. H., 1979, "Free Convective Heat Transfer From Vertical Cylinders With Exposed Ends," Trans. Can. Soc. Mech. Eng., **5**(4), pp. 231–234.
[20] Eslami, M., and Jafarpur, K., 2011, "Laminar Natural Convection Heat Transfer From Isothermal Vertical Cylinders With Active Ends," Heat Transfer Eng., **32**, pp. 506–513.
[21] Yovanovich, M. M., 1987, "On the Effect of Shape, Aspect Ratio and Orientation Upon Natural Convection From Isothermal Bodies of Complex Shape," *Convective Transport*, Winter Annual Meeting of the American Society of Mechanical Engineers, Boston, MA, ASME HTD, **82**, pp. 121–129.
[22] Lee, S., Yovanovich, M. M., and Jafarpur, K., 1991, "Effects of Geometry and Orientation on Laminar Natural Convection From Isothermal Bodies," J. Thermophys. Heat Transfer, **5**, pp. 2208–2216.
[23] Churchill, S., and Churchill, R., 1975, "A Comprehensive Correlating Equation for Heat and Component Transfer by Free Convection," AICHE J., **21**, pp. 604–606.
[24] Yovanovich, M., 1987, "New Nusselt and Sherwood Numbers for Arbitrary Isopotential Geometries at Near Zero Peclet and Rayleigh Numbers," Proceedings of the 22nd Thermophysics Conference, AIAA, Honolulu, HI.
[25] Kitamura, K., and Kimura, F., 2008, "Fluid Flow and Heat Transfer of Natural Convection Over Upward-Facing, Horizontal Heated Circular Disks," Heat Transfer–Asian Res., **6**, pp. 339–351.
[26] Kobus, C., and Wedekind, G., 2001, "An Experimental Investigation Into Natural Convection Heat Transfer From Horizontal Isothermal Circular Disks," Int. J. Heat Mass Transfer, **44**, pp. 3381–3384.